

## PULSED NONLINEAR ACOUSTIC FIELDS FROM CLINICALLY RELEVANT SOURCES: NUMERICAL CALCULATIONS AND EXPERIMENTS RESULTS

Janusz WÓJCIK, Tamara KUJAWSKA, Andrzej NOWICKI

Institute of Fundamental Technological Research  
Polish Academy of Sciences  
Świętokrzyska 21, 00-049 Warszawa, Poland  
e-mail: tkujaw@ippt.gov.pl

*(received June 15, 2008; accepted October 19, 2008)*

The goal of this work was to verify experimentally the applicability of the recently developed Time-Averaged Wave Envelope (TAWEn) method [1] as a tool for fast prediction of pulsed nonlinear pressure fields from focused nonaxisymmetric acoustic sources in attenuating media. The experiments were performed in water at the fundamental frequency of 2.8 MHz for spherically focused (focal length  $F = 80$  mm) square ( $20 \times 20$  mm) and rectangular ( $10 \times 25$  mm) sources similar to those used in the design of 1D linear arrays operating with ultrasonic imaging systems. The experimental results obtained with 10-cycle tone bursts at three different excitation levels corresponding to linear, moderately nonlinear and highly nonlinear propagation conditions (0.045, 0.225 and 0.45 MPa on-source pressure amplitude, respectively) were compared with those yielded using the TAWEn approach. Comparison of the experimental and numerical calculations results has shown that the TAWEn approach is well suited to predict (to within  $\pm 1$  dB) both the spatial-temporal and spatial-spectral pressure variations in the pulsed nonlinear acoustic beams.

**Keywords:** rectangular focused apertures, pulsed acoustic fields, nonlinear distortion, numerical modelling and experiments.

### 1. Introduction

A majority of currently used ultrasound imaging systems employs linear arrays, which launch an interrogating wave into tissue by sequential activation of a square or rectangular subsection of the array. However, there are relatively few papers published which consider nonlinear sound beams in attenuating media emitted from sources with the nonaxisymmetric aperture. Also, they provide field modelling for the continuous wave excitation.

## 2. Numerical model

The numerical model used for describing the nonlinear waveform distortion of the pulsed finite-amplitude sound pressure wave propagating through a thermoviscous medium was comprehensively described in [1]. The model was made computationally efficient by means of replacing the Fourier-series solution approach by Time-Averaged Wave Envelope algorithm. The TAWE approach is based on decomposition of the propagating, nonlinearly distorted acoustic pulse or tone burst into a series of sinusoidal pulses with carrier frequencies being the harmonics of the initial (undistorted) acoustic tone burst and with envelopes being the product of two specific functions. The first function represents the solution to the nonlinear wave equation under linear propagation conditions whereas the second function accounts for nonlinear interactions of harmonic components under given boundary conditions. The model is semi-empirical. In order to predict fields generated by considered transducers an apodisation function in analytical form  $f(x, y) = P_0 |1 - (x/a)^m| \cdot |1 - (y/b)^m|$  was introduced. This function produced the transverse pressure distributions in both the  $x$  and  $y$  directions close to the radiating aperture that best reproduced the data measured.

## 3. Materials and methods

### 3.1. Experimental set-up

The experimental set-up used for the measurements is shown in Fig. 1. All measurements were performed at 25°C in temperature-controlled degassed distilled water using two spherically focused piezoelectric transducers made of Pz27 ceramics (Ferroperm, Denmark) having geometrical focal length  $F$  of 80 mm and operating at the resonance frequency of 2.8 MHz. This frequency is frequently used in clinical imaging as it allows both cardiac (fundamental) and abdomen (2nd harmonic) imaging. In addition, it was selected to maximise the number of experimentally generated harmonics that could be quantified using 40 MHz calibrated membrane hydrophone (model 805, Sonora Medical Systems, Inc. Longmont, CO, USA).

The amplitude of the measured harmonics was determined at a given frequency using hydrophone sensitivity ( $V/\mu\text{Pa}$ ) and compared with the corresponding, TAWE algorithm calculated one. The design of the transducers mimicked that of ultrasound imaging array sub-sections. One of the transducers was square ( $a_g = b_g = 20$  mm) and the other one rectangular ( $a_g = 10$  mm,  $b_g = 25$  mm). Both transducers were backed and had a quarter-wavelength matching layer to optimise transmitting efficiency. As already mentioned, the pressure field generated by the transducers was measured using a broadband bilaminar polyvinylidene difluoride (PVDF) membrane hydrophone (Sonora Medical Systems Inc. SN S5-153, preamplifier P-159, Longmont, CO, USA) with an effective diameter of the sensor element of 0.414 mm and calibrated up to 40 MHz. The transmitting transducer was mounted in the mechanical positioning system driven by three stepper motors allowing its motion in the  $x$ ,  $y$ ,  $z$  directions with

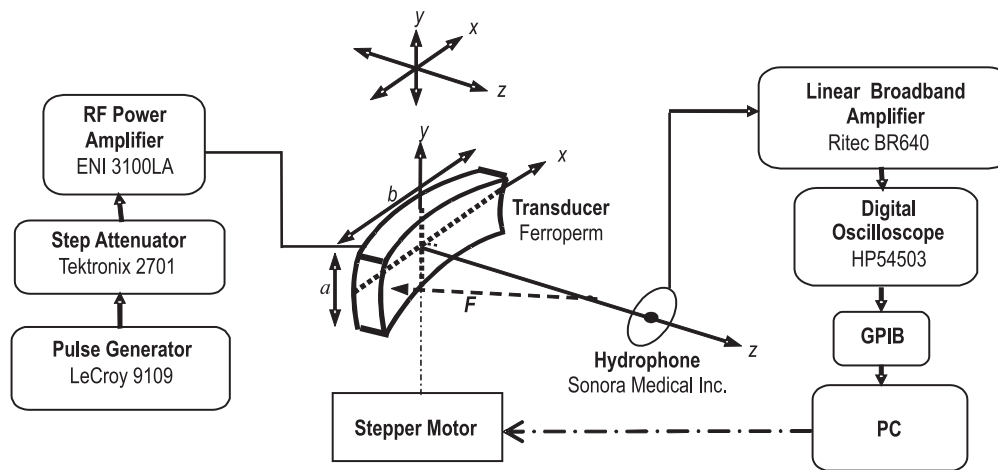


Fig. 1. Schematic diagram of the experimental set-up.

steps adjustable from 0.1 to 5 mm. The  $xyz$  micromanipulator allowed also its rotation in azimuth. The measuring hydrophone was fixed. To maximise the signal to noise ratio at the measurement of the 14th harmonic the tested transducers were driven by 10-cycle tone bursts via RF Power Amplifier (ENI 3100LA, Rochester, NY, USA). The amplitude of the tone burst excitation voltage was controlled by the Step Attenuator (Tektronix 2701, Beaverton, OR, USA) in order to enable linear, moderately nonlinear and highly nonlinear wave distortion. The frequency and duration of the tone bursts were adjustable using Arbitrary Function Generator (LeCroy 9109, Chestnut Ridge, NY, USA). As described below at the low excitation level the sources produced surface pressure of 0.045 MPa. Moderately and highly nonlinear fields were produced by enhancing voltage at the output of the RF amplifier by a factor of 5 (producing surface pressure of 0.225 MPa) and 10 times (producing surface pressure of 0.45 MPa), respectively. The hydrophone output was additionally amplified by 20 dB using the linear broadband amplifier (Ritec BR-640, Warwick, RI, USA) and then fed to the input of an 8-bit digital oscilloscope (HP54503A, Hewlett Packard, Colorado Springs, CO, USA) with a 200 MHz sampling frequency. The received signals were digitised and averaged over 16 consecutive waveforms in the oscilloscope memory and then transferred for spectral analysis to 1.5 GHz clock frequency, 32-bit processor PC laptop with 2 GB RAM. The amplitude of the measured harmonic components was corrected for the hydrophone sensitivity dependence on frequency.

### 3.2. Methodology of measurements

As noted above three excitation levels were used. Initially, the measurements were carried out at low excitation level (linear propagation mode). This was done for each of the tested sources in order to determine the input parameters to the numerical model. These parameters included the speed of sound in water, actual focal length  $F$ , pressure

amplitude  $P_0$  at the transducer surface (source pressure), initial pressure-time waveform and apodisation function. The apodisation function and pressure amplitude  $P_0$  at the transducer surface were determined at low (45 kPa) excitation level by measuring the transverse pressure distributions and their maxima in both the  $x$  and  $y$  directions close to the radiating surface (5–15 mm axial distance). Specifically, the measured axial and lateral pressure distributions were compared with those theoretically predicted using the linear propagation theory and accounting for attenuation while keeping the source pressure  $P_0$  constant and varying the radiating aperture dimensions  $a$ ,  $b$  and exponent  $m$  of the apodisation function (see Sec. 2). At higher excitation levels (here, 225 and 450 kPa) the value of  $P_0$  was scaled up directly proportional to the increase in the applied excitation voltage (5 and 10 times). Figure 2 shows the apodisation function for the square aperture at low excitation level in the  $x$  direction, described by the polynomial  $f(x, 0) = P_0|1 - (x/a)^8|$ , which produced the transverse pressure distribution calculated at the axial distance 15 mm that best fitted to the measured one at the same distance. Here  $a$  and  $b$  are the transducer effective dimensions in both the  $x$  and  $y$  directions,  $m$  is positive integer number that was determined by iteration process. The effective aperture dimensions were found to be  $19 \times 19$  mm for the square and  $24 \times 9$  mm for the rectangular transducer, respectively. Water density and sound speed input to the TAW model corresponded to those at  $25^\circ\text{C}$ , i.e.  $1000 \text{ kg/m}^3$  and  $1497 \text{ m/s}$ , respectively. The frequency-dependent attenuation was introduced into the numerical model as  $\alpha(f) = \alpha_1 f^2$ , where  $\alpha_1 = 2.5 \cdot 10^{-2} \text{ Np/(m}\cdot\text{MHz}^2)$  is the attenuation coefficient at 1 MHz. The nonlinearity parameter of water  $B/A = 5.3$  was used.

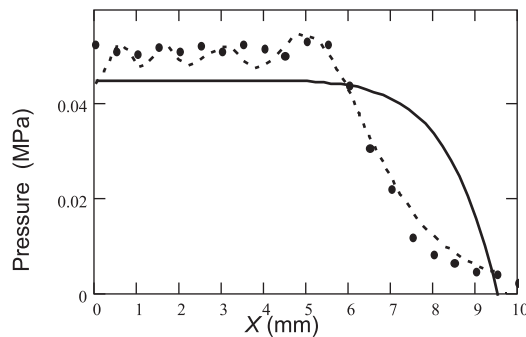


Fig. 2. Square aperture, low excitation level. Solid line: apodisation function assumed for numerical calculations:  $f(x, 0) = P_0 \cdot |1 - (x/a)^8|$  for  $0 \leq x \leq a$  at the radiating aperture surface in the  $x$  (or  $y$ ) direction. Dashed line: the transverse pressure distribution calculated for the above apodisation function at the axial distance of 15 mm and measured at the same distance (dots).

#### 4. Results and discussion

Figures 3–7 show the comparison between the measured pulsed nonlinear acoustic fields (dots) and their theoretical predictions (solid lines) obtained using the TAW model approach for both transducers tested.

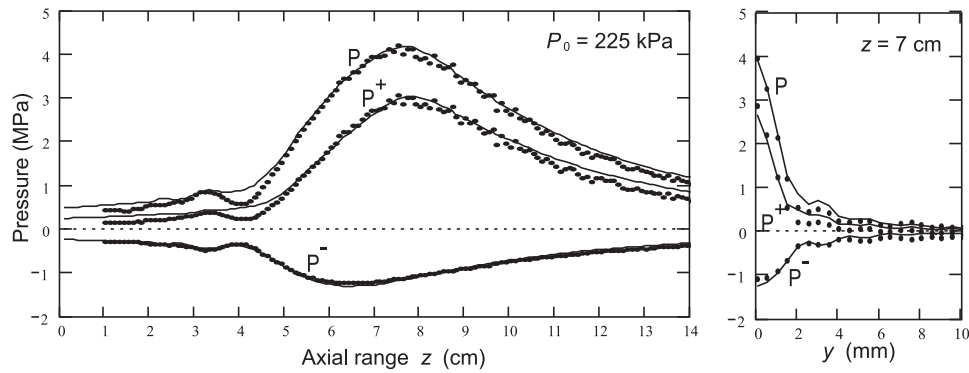


Fig. 3. Square aperture, moderate excitation level. Pressure distributions for the peak-compression ( $P^+$ ), peak-rarefaction ( $P^-$ ) and peak-to-peak ( $P$ ) amplitudes. Solid lines: predicted. Dots: measured. Left: axial pressure distributions. Right: lateral distributions in the plane  $z = 7$  cm.

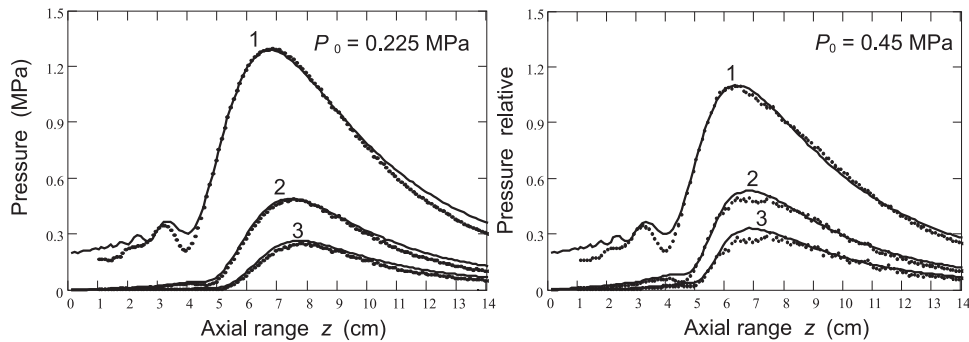


Fig. 4. Square aperture, moderate (left) and high (right) excitation level. Axial pressure distributions for 2.8 MHz fundamental (1), second (2) and third (3) harmonics. Solid lines: numerically predicted. Dots: measured.

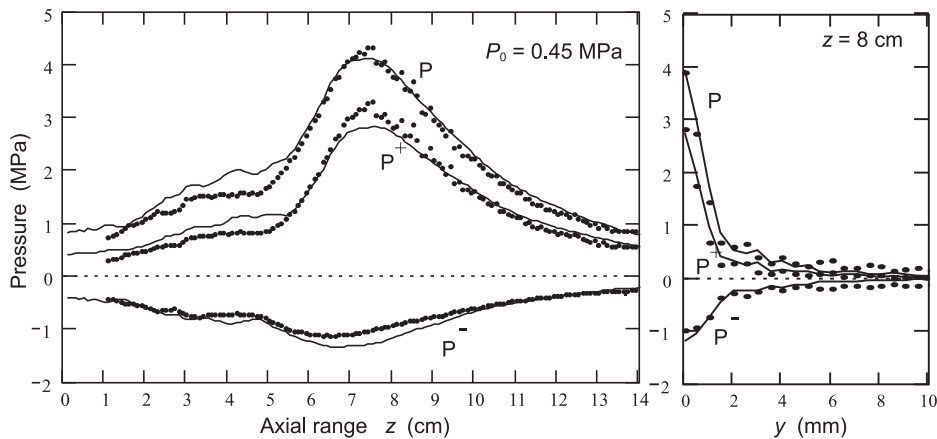


Fig. 5. Rectangular aperture, high excitation level. Pressure distributions for the peak-compression ( $P^+$ ), peak-rarefaction ( $P^-$ ) and peak-to-peak ( $P$ ) amplitudes. Solid lines: predicted. Dots: measured. Left: axial pressure distributions. Right: lateral distributions in the plane  $z = 8$  cm.

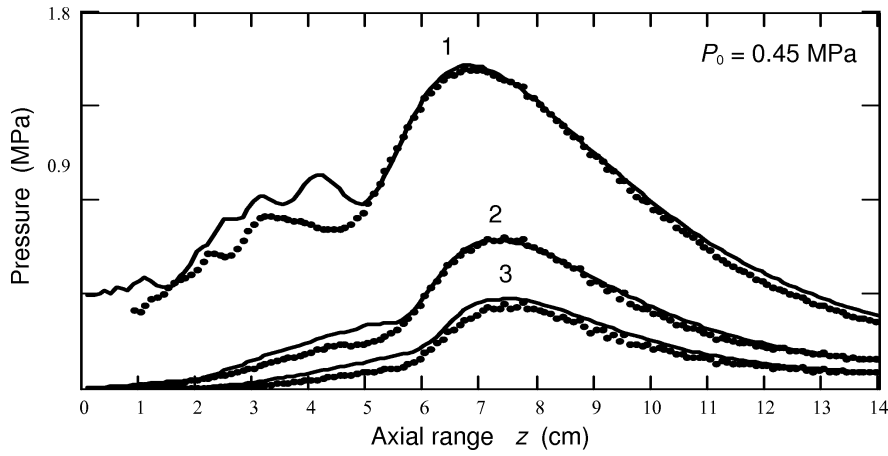


Fig. 6. Rectangular aperture, high excitation level. Axial pressure distributions for 2.8 MHz fundamental (1), second (2) and third (3) harmonics. Solid lines: predicted. Dots: measured.

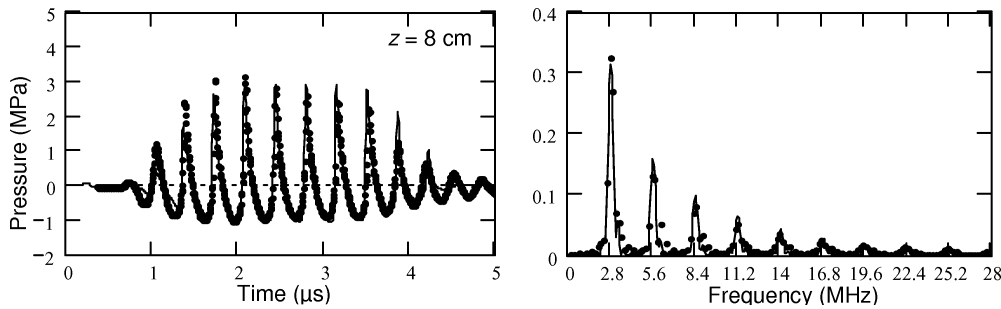


Fig. 7. Rectangular aperture, high excitation level. Pressure-time waveforms and their spectra of 10-cycle tone burst on the axis at the focal plane. Solid lines: predicted. Dots: measured.

## 5. Conclusions

The comparison of the experimental results and numerical predictions has shown that the TAW approach is capable of predicting correctly both the spatial-temporal and spatial-spectral pressure distributions. The discrepancies (within  $\pm 1$  dB) between the theoretically predicted pressure distributions and those determined experimentally, were probably caused by the finite aperture of the hydrophone sensitive element and the uncertainty of the hydrophone calibration.

## Acknowledgments

This work was supported by the Ministry of Science and Higher Education (Grant No 518 002 32/0219, period 2007–2009). There is the extended version of the paper presented at the 55th Open Seminar on Acoustics, Piechowice 2008.

## References

- [1] WÓJCIK J., NOWICKI A., LEWIN P.A., BLOOMFIELD P.E., KUJAWSKA T., FILIPCZYŃSKI L., *Wave envelopes method for description of nonlinear acoustic wave propagation*, *Ultrasonics*, **44**, 310–329 (2006).
- [2] CHRISTOPHER P.T., PARKER K.J., *New approaches to nonlinear diffractive field propagation*, *J. Acoust. Soc. Am.*, **90**, 1, 488–499 (1991).
- [3] KAMAKURA T., TANI M., KUMAMOTO Y., *Harmonic generation in finite amplitude sound beams from a rectangular aperture source*, *J. Acoust. Soc. Am.*, **91**, 6, 3144–3151 (1992).
- [4] BAKER A.C., BERG A.M., SAHIN A., NAZE TJØTTA J., *The nonlinear pressure field of plane, rectangular apertures. Experimental and theoretical results*, *J. Acoust. Soc. Am.*, **97**, 6, 3510–3517 (1995).
- [5] NACHEF S., CATHIGNOL D., NAZE TJØTTA J., BERG A.M., TJØTTA S., *Investigation of a high intensity sound beam from a plane transducer. Experimental and theoretical results*, *J. Acoust. Soc. Am.*, **98**, 4, 2303–2323 (1995).
- [6] CAHILL M.D., BAKER A.C., *Increased off-axis energy deposition due to diffraction and nonlinear propagation of ultrasound from rectangular sources*, *J. Acoust. Soc. Am.*, **102**, 1, 199–203 (1997).
- [7] CAHILL M.D., BAKER A.C., *Numerical simulation of the acoustic field of a phased-array medical ultrasound scanner*, *J. Acoust. Soc. Am.*, **104**, 3, 1274–1283 (1998).
- [8] ZEMP R.J., TAVAKKOLI J., COBBOLD R.S.C., *Modeling of nonlinear ultrasound propagation in tissue from array transducers*, *J. Acoust. Soc. Am.*, **113**, 1, 139–152 (2003).